

Improved design of transversally stiffened steel plate girders subjected to patch loading

Rolando Chacón^a, Juan Herrera^a, Luis Fargier-Gabaldón^b

^aDepartment of Civil and Environmental Engineering
Universitat Politècnica de Catalunya, Barcelona, Spain

^bDepartamento de Estructuras
Universidad de los Andes, Mérida, Venezuela

Abstract

This article presents a mechanical formulation to estimate the strength of transversally stiffened steel plate girders subjected to patch loading, in this particular case, with closely spaced stiffeners. Steel plate girders with closely spaced stiffeners are occasionally found in bridge design and for such cases, the current EN1993-1-5 rules underestimate the strength of the webs to transverse forces. A FE-based parametric investigation is conducted to estimate the web strength to patch loading. The results are compared to the results obtained from classical beam theory in combination with the proposed formulation. A notional plate girder is analyzed to demonstrate the potential of the formulation for daily routine designs. Results indicate that the proposed formulation does a better job in predicting the web strength of transversely stiffened girders subjected to patch loading than the EN1993-1-5 specification, and thus yield a lighter and more economical design for these specific girder geometries.

Notation

h_w	clear web depth between flanges
t_w	web thickness
t_f	flange thickness
t_s	transverse stiffener thickness
b_f	flange width
a	length of a stiffened or unstiffened plate
L_{eff}	effective length for resistance
l_y	effectively loaded length
σ_f	longitudinal stresses in the flanges
k_F	buckling coefficient
χ_F	reduction factor due to local buckling
λ_F	plate slenderness
f_{yf}	flange yield stress
f_{yw}	web yield stress
s_s	length of stiff bearing
F_{Rk}	Characteristic design resistance to local buckling under transverse forces
N_{Ed}	design axial force
F_{Ed}	design transverse force
V_{Ed}	design shear force
M_{Ed}	design bending moment

1. Introduction

The incremental launching method as a constructive process of bridges has had a great boom since the second half of the twentieth century. It allows to significantly optimize time-constraints and to reduce auxiliary support elements. Bridges assembled with steel plate girders are ideal for this construction process due to their reduced weight and ease of maneuverability. Steel plate girders are built by assembling thin-walled elements in which the web slenderness ratio, defined as h_w/t_w , ranges from 80 (stocky) to 250 (slender). Because of the high slenderness ratios of the web, it is common practice to provide a considerable amount of transverse and/or longitudinal stiffening to avoid instability-related phenomena due to compressive, shear and concentrated forces, or their combination, during construction and / or service lifespan of the structure.

Launching minimizes the use of heavy equipment and implies that all cross-sections of the plate girder pass over temporary supports or piers and thus, concentrated forces act in both stiffened and unstiffened sections. Occasionally, t_w is governed by a temporary concentrated load during the launching operation.

An alternative to increasing the web thickness is to stiffen the web plate with equally spaced vertical stiffeners or a combination of vertical and longitudinal stiffeners. Vertical stiffeners are spaced a distance "a", ranging from $a/h_w=1.0$ to $a/h_w=4.0$. Engineering judgement suggests that the smaller the distance "a", the higher the buckling strength of the web plate. However, the EN1993-1-5 [1] design provision shows that for spacing less than $a/l_y=1$, the predicted strength of the web reduces with the reduction of the spacing between vertical stiffeners (a), as shown in Fig 1.

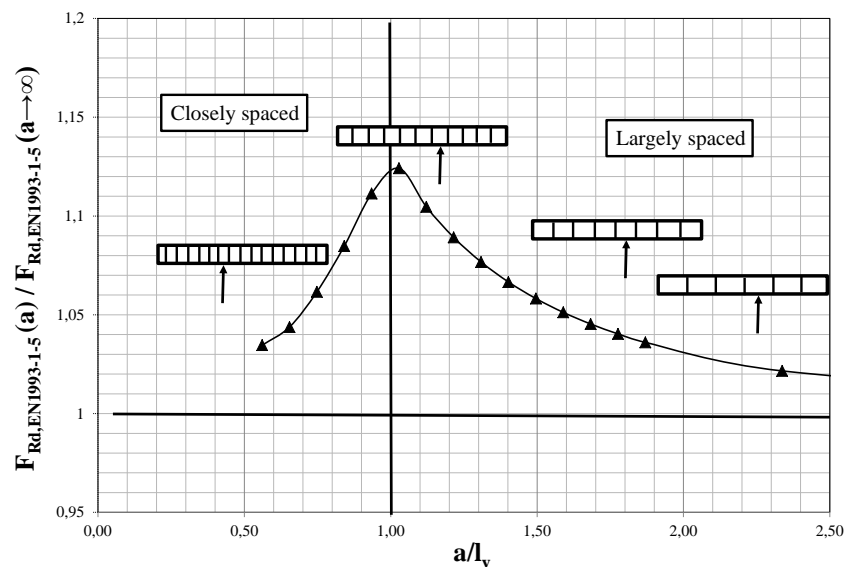


Figure 1. EN1993-1-5 resistance to transverse forces as a function of a/l_y

The ultimate strength of steel plate girders subjected to patch loading has been studied in depth for members with largely spaced stiffeners ($a/l_y > 1.0$) through mechanical models [2-3], critical buckling loads approaches [4-5], bending and shear interaction schemes [6-8] and more recently, bridge launching Structural Health Monitoring (SHM) applications have been implemented [9-10]. The case of closely spaced stiffeners has been studied to a lesser extent both experimentally and numerically, except for the work reported in References [11, 13] and the design formulation summarized in [12]. This formulation has been calibrated with experimental results with a satisfactory level of accuracy. However, as it will be explained later, the formulae provided in [12] is a function of the stresses in the flange of the plate girder (σ_f), which are obtained through a 3D model such as complex brick- or shell-based Finite Element (FE) simulations, thus reducing its practical application for daily routing designs. In this paper, practical applications of the formulation presented in [12] are proposed in which the stresses in the flange (σ_f) are calculated with the classical beam theory and compared to the results of a 3D shell-based FE-simulation. On the other hand, recent research in the field has been focused on longitudinally stiffened plates and eccentric concentrated loading [14-16].

2. Formulation of EN1993-1-5 to transverse forces

The prediction of the ultimate load carrying capacity of plate girders subjected to concentrated loads (F_{Rk}) is included in EN1993-1-5 in the same form as in other instability-related problems, i.e., the χ - λ approach Eq. (1-3). In this approach, the plastic strength F_y is partially reduced by χ_F (Eq. 3). l_y is calculated from geometrical and material magnitudes (Eq. 2). Note that the magnitude of l_y is limited to the distance “a”. As a consequence, the ultimate load carrying capacity given by the F_{Rk} in EN1993-1-5 specification yields a reduction in the strength of the web of the plate girder as the spacing “a” between vertical stiffeners is reduced below l_y .

$$F_{Rk} = \chi_F \cdot F_y = \chi_F \cdot f_{yw} \cdot l_y \cdot t_w \leq \chi_F \cdot f_{yw} \cdot a \cdot t_w \quad (1)$$

$$l_y = S_s + 2 \cdot t_f \cdot \left(1 + \sqrt{m_1 + m_2}\right) = S_s + 2 \cdot t_f \cdot \left(1 + \sqrt{\frac{f_{yf} \cdot b_f}{f_{yw} \cdot t_w} + 0,02 \cdot \left(\frac{h_w}{t_f}\right)^2}\right) \leq a \quad (2)$$

$$\chi_F = \frac{0,5}{\lambda_F} \quad \bar{\lambda}_F = \sqrt{\frac{F_y}{F_{cr}}} \quad F_{cr} = 0,9 \cdot k_f \cdot E \cdot \frac{t_w^3}{h_w} \quad (3)$$

It is important to point out that l_y has also been a subject of study within the core of European Committee of Standardization CEN / TC250 / SC3. In future versions of EN1993-1-5, this magnitude will be changed to the one largely described in [17]. The described formulation will also be applicable if the new version of l_y is used.

3. Proposed design formulation

A solution to the problem of web instability in plate girders with closely spaced vertical stiffeners under patch loading can be found on a hinge mechanism, as proposed in Ref. [12]. The proposed model is based on an equation with two terms (Eq. 4). The first term

contains the web contribution given in the EN1993-1-5 specification for $l_y=a$ while the second term is a correction factor designated as ΔF_f .

$$F_{Rk,proposed} = F_{Rk}^* = F_{Rk(l_y=a)} + \Delta F_f = \chi \cdot F_{y(l_y=a)} + \Delta F_f = \chi \cdot f_{yw} \cdot a \cdot t_w + \Delta F_f \quad (4)$$

The derivation of ΔF_f is presented in Ref. [12]. A yield mechanism analysis was used, which involves the formation of four plastic hinges in the loaded flange of the steel plate girder. It is assumed that the web folds at a load of magnitude F_1 (Fig. 2). Thus, further load increments are resisted by the loaded flange which acts as a flat-beam with cross-section $b_f \cdot t_f$ subjected to bending. If the transverse stiffeners are rigid, the flat-beam can be approximated as fully restrained element at both ends and the total length of this member equals to the distance between transverse stiffeners “a”. The flexural resistance of the flange is calculated by considering the flange cross-section $b_f \cdot t_f$ only (Eq. 5). However, because of bending due to external loads, axial stresses are present in the flange during the launching operation, and thus, only a fraction of the nominal yield strength of the flange (f_{yf}) defined as f_{yf}^* , is used in the mechanism analysis.

The magnitude f_{yf}^* is the available yield strength reserve at a transverse force equals to F_1 (Fig. 2). The magnitudes of χ_{fi} and χ_{fo} (Eq. 6) represent the ratio of actual longitudinal stress in the flange (σ_{fj}) obtained from 3D shell-based FE models to the nominal yield stress (f_{yf}), for each hinge at F_1 [12]. The magnitude of ΔF_f accounts for the flange contribution to the web strength and is obtained using the principle of virtual work in a four hinge model of a flat beam (Eq. 7). The internal energy dissipated by the hinges (M_{yf}) is equaled to the applied energy from external loads. The coefficient k (Eq. 8) has been proposed from empirical calibrations in subsequent publications presented by the authors in order to account for the design of hybrid plate girders [13].

$$M_{yf} = \frac{1}{4} b_f \cdot t_f^2 \cdot f_{yf}^* \quad (5)$$

$$f_{yf,o}^* = (1 - \chi_{fo}) \cdot f_{yf} \quad f_{yf,i}^* = (1 - \chi_{fi}) \cdot f_{yf} \quad \chi_{fj} = \frac{\sigma_j}{f_{yf}} \left(1.0 + 0.005 \left(\frac{h_w}{t_w} \right) \right) \quad (6)$$

$$\Delta F_f = \frac{b_f \cdot t_f^2 \cdot f_{yf}}{(a - S_s)} [2 - (\chi_{fo} + \chi_{fi})] \quad (7)$$

$$k = \left[1.25 - 0.25 \left(\frac{f_{yf}}{f_{yw}} \right) \right] \quad (8)$$

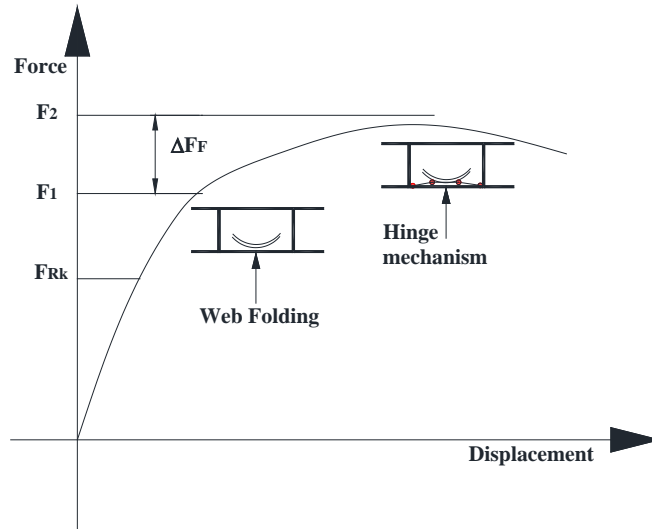


Figure 2. Load-displacement response plot for girders with closely spaced stiffeners

This investigation is focused on the numerical reproduction of full-scale symmetric steel plate girders with closely spaced stiffeners subjected to concentrated loading. As an example of potential applications, consider a plate girder continuous beam over four supports, with 20-30-20-meter span arrangement (Fig. 3). During launching, the stage just before touchdown of the steel girder at the second intermediate pier is likely to dictate the thickness of the web under patch loading and thus is chosen as the most critical design case. At this location, the section of the girder over the first pier carries significant bending moment and shear. For this case, a parametric analysis was conducted for different combinations of t_w , t_s , f_{yf} and s_s . Stresses in the flange were obtained through linear elastic analyses using classical beam theory which were compared to the stresses obtained through fully Geometrically and Materially Nonlinear Analyses with Imperfections included (GMNIA). The latter were developed in Abaqus Simulia [18] with shell elements, following the recommendations described in Annex-C of [1] in which the material was defined as elastic perfectly plastic. In this Annex, two types of analysis are suggested: i) a refined analysis including both geometrical eigenvalue-based initial shapes and structural imperfection due to plate cutting and welding and ii) an equivalent analysis in which a combination of only geometrical imperfections are modeled. In this particular case, based upon a vaster comparison between experimental and numerical results previously depicted in [19], the numerical modeling followed the characteristics described as follows:

- The imperfection shape was based upon the first eigenmode obtained in a previous buckling analysis. This mode was fully related to local buckling of the directly loaded panel.
- This shape was scaled to an imperfection magnitude of 80% of the fabrication tolerances, which for plates is related to the minimum between $h_w/100$ and t_w .
- A residual stress pattern was included. In this case, a residual stress pattern suggested by the BSK 99 [20] (Swedish design manual on steel construction) was included as an initial structural imperfection.

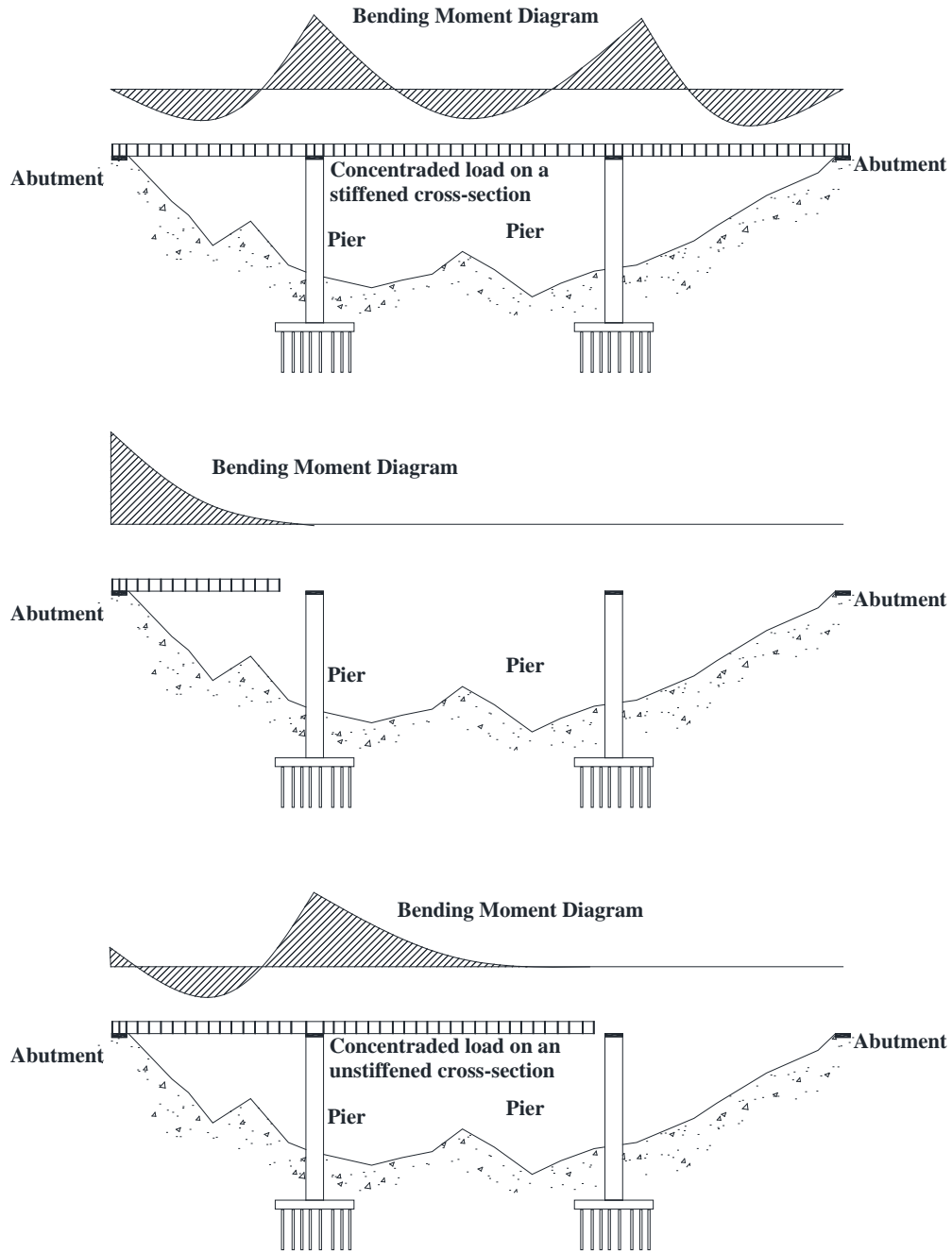


Figure 3. Structural design situations to be considered during bridge launching.

A summary of the geometry and material properties used in the parametric investigation is summarized in Table 1. A total 144 and 24 simulations were conducted, using the 3D, FE GMNIA and the simple beam model, respectively. Note that for beam models the bearing length s_s cannot be included as a variable parameter.

	Beam elements	Shell elements												
Analysis	LA	GMNIA												
h_w (mm)	1500	1500												
a (mm)	1500	1500												
b_f (mm)	500	500												
f_{yw} (N/mm ²)	355	355												
f_{yf} (N/mm ²)	355	355 460 690												
s_s (mm)	0	375 750												
t_w (mm)	<table border="1" style="margin: auto;"> <tr><td style="padding: 2px;">5</td><td style="padding: 2px;">6</td></tr> <tr><td style="padding: 2px;">8</td><td style="padding: 2px;">10</td></tr> <tr><td style="padding: 2px;">12</td><td style="padding: 2px;">15</td></tr> </table>	5	6	8	10	12	15	<table border="1" style="margin: auto;"> <tr><td style="padding: 2px;">5</td><td style="padding: 2px;">6</td></tr> <tr><td style="padding: 2px;">8</td><td style="padding: 2px;">10</td></tr> <tr><td style="padding: 2px;">12</td><td style="padding: 2px;">15</td></tr> </table>	5	6	8	10	12	15
5	6													
8	10													
12	15													
5	6													
8	10													
12	15													
t_s (mm)	<table border="1" style="margin: auto;"> <tr><td style="padding: 2px;">12</td><td style="padding: 2px;">15</td></tr> <tr><td colspan="2" style="padding: 2px;">only in weight</td></tr> <tr><td style="padding: 2px;">20</td><td style="padding: 2px;">30</td></tr> </table>	12	15	only in weight		20	30	<table border="1" style="margin: auto;"> <tr><td style="padding: 2px;">12</td><td style="padding: 2px;">15</td></tr> <tr><td style="padding: 2px;">20</td><td style="padding: 2px;">30</td></tr> </table>	12	15	20	30		
12	15													
only in weight														
20	30													
12	15													
20	30													
Total	24	144												
Results	Flange stress levels	Full response P-6												

Table 1. Parametric study for beam and Shell models

4. Results

4.1 Shell-based geometries

Figure 4 shows the load versus displacement response for web thickness of 5, 10, 15 mm, which correspond to very slender, moderately slender and stocky girders, respectively. A similar response is observed in all cases. To facilitate the interpretation of results, the EN1993-1-5 characteristic resistance F_{Rk} is added as a horizontal marker. The results summarized in Figure 4 suggest:

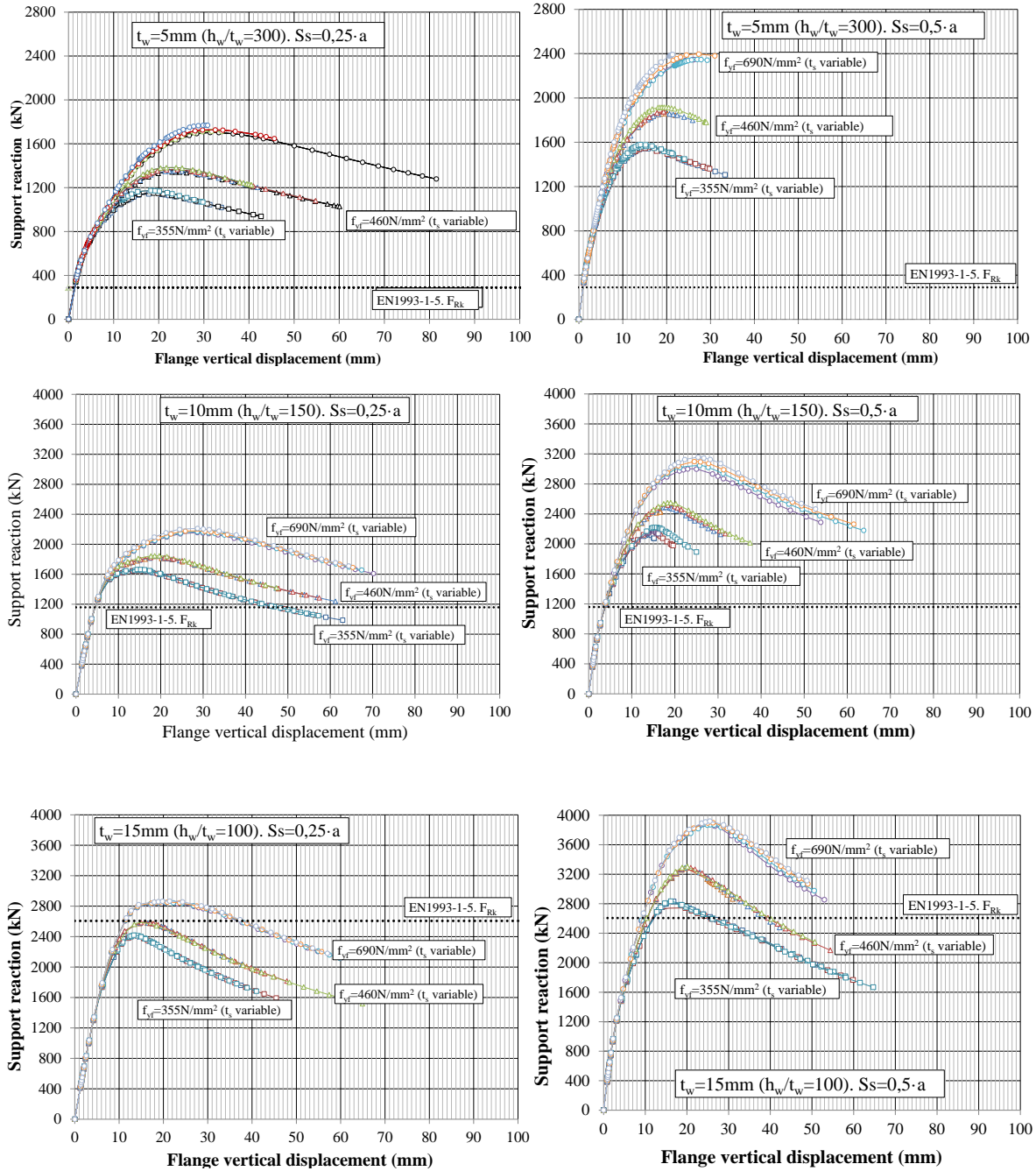


Figure 4. Structural P- δ response for values of t_w (top to bottom) and s_s/a (left to right)

- The EN1993-1-5 significantly underestimates the strength of very slender in plate girder ($h_w/t_w=300$) under concentrated forces.
- The yield strength of the flange has a significant impact in the web strength under patch loading. Note that hybrid girders with $f_{yf}=460 \text{ N/mm}^2$ and $f_{yf}=690 \text{ N/mm}^2$ show an increase in the strength when compared to their homogeneous counterparts with $f_{yf}=f_{yw}=355 \text{ N/mm}^2$

- As expected, the increase in the support length leads to an increase in the beam strength under patch loading.
- The influence of the stiffener thickness in the strength of plate girders under patch loading was found negligible for design purposes if the element accomplishes the stiffness requirements of EN1993-1-5. In this particular case, t_s ranged from 15 mm to 30 mm.
- The EN1993-1-5 over predicts the buckling strength of the web for stocky plate girders in which $f_{yf}=355 \text{ N/mm}^2$. In these cases, the 3D, FE GMNIA simulation showed web folding with considerable web yielding, without the formation of the four-hinge mechanism in the flat beam.

t_w (mm)	S_s/a	f_{yf} (N/mm ²)	$F_{Rk(l_y=a)}$ (kN)	F_2 (kN)	σ_{fi}	σ_{fo}	κ	χ_{fi}	χ_{fo}	ΔF_f (kN)	F_{Rk}^* (kN)	F_2/F_{Rk}	F_2/F_{Rk}^*	
5	0,25	355	289,60	1155,56	48,45	31,99	1,00	0,34	0,23	814,24	1103,84	3,99	1,05	
		460		1359,64			0,93	0,26	0,17	1065,19	1354,79	4,69	1,00	
		690		1726,85			0,76	0,18	0,12	1441,25	1730,85	5,96	1,00	
	0,50	355		1557,34	58,09	31,99	1,00	0,41	0,23	1163,52	1453,12	5,38	1,07	
		460		1876,14			0,93	0,32	0,17	1544,22	1833,82	6,48	1,02	
		690		2370,61			0,76	0,21	0,12	2117,68	2407,28	8,19	0,98	
6	0,25	355	417,03	1235,90	71,02	47,21	1,00	0,45	0,30	710,37	1127,40	2,96	1,10	
		460		1437,31			0,93	0,35	0,23	969,00	1386,02	3,45	1,04	
		690		1818,72			0,76	0,23	0,15	1361,88	1778,91	4,36	1,02	
	0,50	355		1648,83	84,81	47,21	1,00	0,54	0,30	991,09	1408,12	3,95	1,17	
		460		1975,45			0,93	0,41	0,23	1384,54	1801,56	4,74	1,10	
		690		2539,38			0,76	0,28	0,15	1985,93	2402,95	6,09	1,06	
8	0,25	355	741,38	1419,56	123,19	74,96	1,00	0,67	0,41	521,74	1263,11	1,91	1,12	
		460		1612,02			0,93	0,52	0,32	794,31	1535,69	2,17	1,05	
		690		1988,76			0,76	0,35	0,21	1217,75	1959,13	2,68	1,02	
	0,50	355		1868,40	136,56	74,96	1,00	0,75	0,41	720,43	1461,81	2,52	1,28	
		460		2199,36			0,93	0,58	0,32	1133,89	1875,27	2,97	1,17	
		690		2807,23			0,76	0,38	0,21	1779,12	2520,50	3,79	1,11	
10	0,25	355	1158,40	1651,26	153,71	97,67	1,00	0,76	0,48	432,14	1590,54	1,43	1,04	
		460		1822,70			0,93	0,58	0,37	711,34	1869,74	1,57	0,97	
		690		2176,15			0,76	0,39	0,25	1149,29	2307,69	1,88	0,94	
	0,50	355		2173,13	191,75	97,67	1,00	0,95	0,48	488,44	1646,84	1,88	1,32	
		460		2495,00			0,93	0,73	0,37	919,05	2077,46	2,15	1,20	
		690		3073,99			0,76	0,49	0,25	1601,85	2760,26	2,65	1,11	
12	0,25	355	1668,10	1951,57	295,50	211,81	1,00	>1,0	n.a.	n.a.	n.a.	n.a.	n.a.	
		460		2097,08			0,93	>1,0	n.a.	n.a.	n.a.	n.a.	n.a.	
		690		2399,85			0,76	0,70	0,50	679,27	2347,37	1,44	1,02	
	0,50	355		2502,27	> f_{yf}	211,81	1,00	n.a.	n.a.	n.a.	n.a.	n.a.	n.a.	n.a.
		460		2816,16			0,93	n.a.	n.a.	n.a.	n.a.	n.a.	n.a.	
		690		3385,26			0,76	0,85	0,50	826,13	2494,23	2,03	1,36	
15	0,25	355	2606,40	2409,71	> f_{yf}		1,00	n.a.	n.a.	n.a.	n.a.	n.a.	n.a.	
		460		2579,39			0,93	n.a.	n.a.	n.a.	n.a.	n.a.	n.a.	
		690		2845,58			0,76	n.a.	n.a.	n.a.	n.a.	n.a.	n.a.	
	0,50	355		2741,20	> f_{yf}		1,00	n.a.	n.a.	n.a.	n.a.	n.a.	n.a.	n.a.
		460		3288,98			0,93	n.a.	n.a.	n.a.	n.a.	n.a.	n.a.	
		690		3871,50			0,76	n.a.	n.a.	n.a.	n.a.	n.a.	n.a.	

Table 2. Results obtained in the Shell-based models.

Numerical results are summarized in Table 2, including the ultimate load carrying capacity, F_2 , based on the 3D FE GMNIA models, the strength prediction obtained as per EN1993-1-5, F_{Rk} and the strength calculated using the proposed formulation $F_{Rk^*} = F_{Rk}(l_y=a) + \Delta F_f$. In Table 2, the flange yield reserve (Eq. 6) is obtained from the 3D FE GMNIA model, as the average flange stress between the vicinity of the flange-to-stiffener joint and the edge of the patch load (Fig. 5). The support reaction is chosen from the incremental analysis such that it approaches F_{Rk} . The corresponding χ_{fi} , χ_{fo} and k factors are included in Table 2. The results summarized in Table 2 suggests:

- Except for cases in which $t_w=15$ mm, the magnitudes of $F_{Rk}(l_y=a)$ are significantly smaller than the calculated F_2 .
- χ_{fi} , χ_{fo} increase with the increase in the web thickness. For the very stocky cases, the flange yield reserve exceeds the nominal yielding stress and thus the formulation is not applicable.
- The proposed formulation ($F_{Rk^*} = F_{Rk}(l_y=a) + \Delta F_f$) in which the stresses in the flange of the plate girder are obtained through the 3D FE GMNIA yield strength ratios (F_2/F_{Rk^*}) between 0.97 to 1.37, while the strength ratio of the current EN1993-1-5 provision (F_2/F_{Rk}) ranges between 1.17 and 8.99.

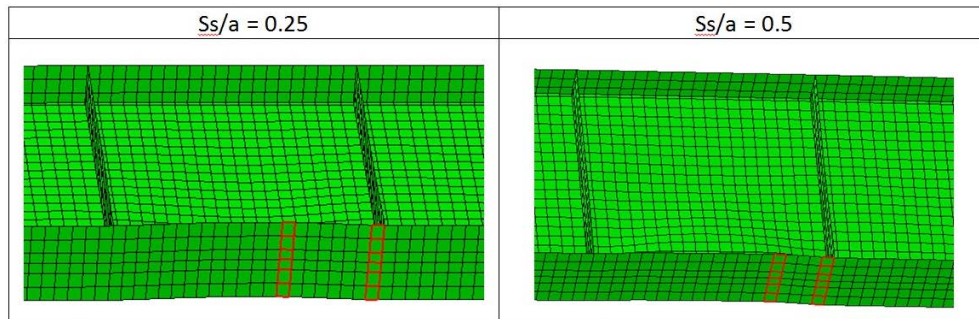


Figure 5. Location of the flange hinge for $s_s/a=0,25$ and for $s_s/a=0,5$.

4.2 Beam-based geometries

The application of the proposed formulation is investigated for the case of simple beam models to calculate the stress in the flange to avoid time-consuming and computationally costly 3D FE GMNIA. The numerical model is based on a two-spanned, two-noded linear beams. External loads acting on the plate girder include self-weight (including vertical stiffeners) and an additional uniformly distributed load such that to produce a reaction of magnitude F_{Rk} at the intermediate support. Fig 6 displays the numerical representation, the bending moment diagram for the considered structural configuration as well as an illustration of the manner from which F_{Rk} is obtained. Values of longitudinal stresses σ are

obtained at approximate locations of where the plastic hinges may form. Bending moment at the support follow from statics and compatibility of deformations and the axial stresses acting on the flange due to bending are hand calculated with the beam theory. Note that the bearing length and its beneficial effect cannot accurately be accounted for in this case. In addition, the beam model does not reproduce the geometrical or structural imperfections. A Timoshenko beam model was developed in Abaqus-Simulia as an alternative to the Euler-Bernoulli formulation to account for shear deformations. Results of the beam model are summarized in Table 3. Note that the flange yield reserves are obtained from the beam model. A comparison of results from tables 2 and 3 suggests:

- The obtained $F_{Rk(l_y=a)}$ for the case of beam models are lower than those obtained through 3D FE GMNIA.
- The magnitude of ΔF_f calculated with simple beam models tend to be slightly larger than those obtained through the 3D FE GMNIA.
- The formulation is not applicable to very stocky webs, as in the case of the analyses using the 3D FE GMNIA.

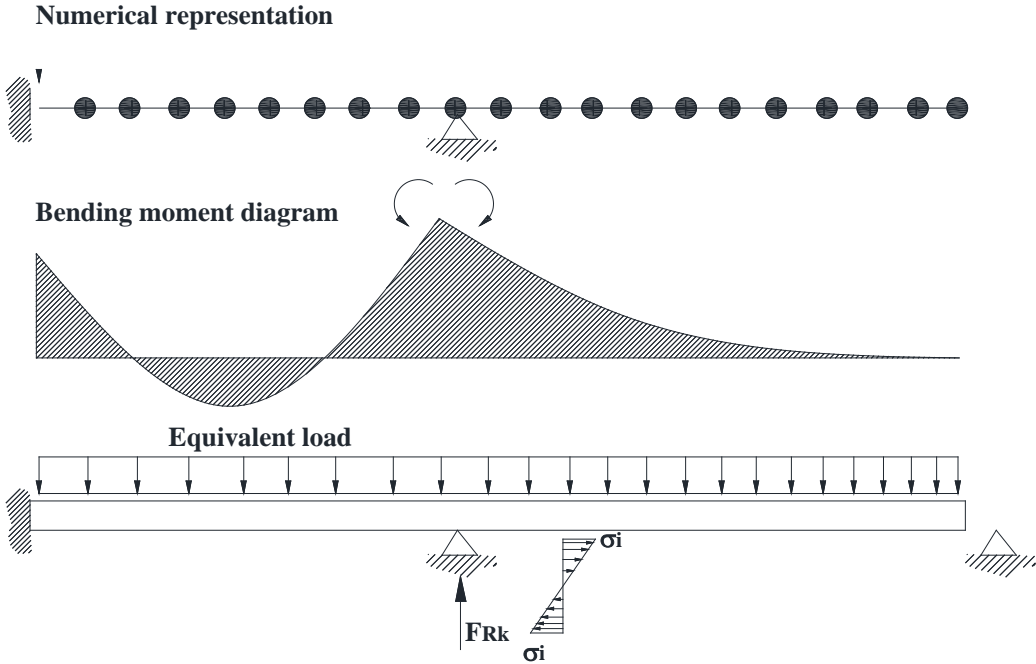


Figure 6. Structural beam model

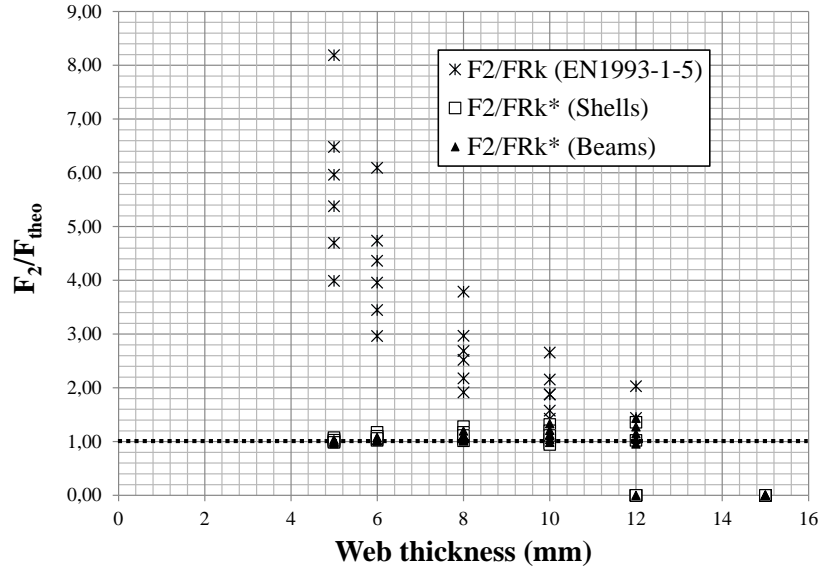


Figure 7. Numerical (F_2) vs- Theoretical (F_{Rk}) ratios for all studied proposals.

Figure 7 shows a plot of three different strength ratios for F_2 . The first ratio is to the EN1993-1-5 current prediction ($F_2/F_{Rk, EN1993-1-5}$), the second ratio is to the proposed formulation using 3D FE GMNIA to infer the flange stresses ($F_2/F_{Rk^*, shell}$), and the third ratio is to the proposed formulation using the Timoshenko beam theory for calculating stress in the flange ($F_2/F_{Rk^*, beam}$). Results suggest that the simplify method to estimate the strength of plate girders under patch loading based on a beam model does a better job than the current EN1993-1-5, specially for the case of plate girders with thin webs, and that the current EN1993-1-5 significantly overestimate the strength of slender plate girders under patch loading.

t_w (mm)	S_s/a	f_{yf} (N/mm ²)	$F_{Rk(ly=a)}$ (kN)	F_2 (kN)	σ_{fi}	σ_{fo}	κ	χ_{fi}	χ_{fo}	ΔF_f (kN)	F_{Rk}^* (kN)	F_2/F_{Rk}	F_2/F_{Rk}^*	
5,00	0,25	355	289,60	1155,56	39,99	36,82	1,00	0,28	0,26	828,77	1118,37	3,99	1,03	
		460		1359,64			0,93	0,22	0,20	1078,64	1368,25	4,69	0,99	
		690		1726,85			0,76	0,14	0,13	1452,35	1741,95	5,96	0,99	
	0,50	355		1557,34	38,92	36,82	1,00	0,27	0,26	1249,60	1539,20	5,38	1,01	
		460		1876,14			0,93	0,21	0,20	1623,93	1913,53	6,48	0,98	
		690		2370,61			0,76	0,14	0,13	2183,45	2473,05	8,19	0,96	
6,00	0,25	355	417,03	1235,90	57,20	52,66	1,00	0,36	0,33	740,52	1157,55	2,96	1,07	
		460		1437,31			0,93	0,28	0,26	996,92	1413,95	3,45	1,02	
		690		1818,72			0,76	0,19	0,17	1384,92	1801,95	4,36	1,01	
	0,50	355		1648,83	55,66	52,66	1,00	0,35	0,33	1119,07	1536,10	3,95	1,07	
		460		1975,45			0,93	0,27	0,26	1503,06	1920,08	4,74	1,03	
		690		2539,38			0,76	0,18	0,17	2083,72	2500,74	6,09	1,02	
8,00	0,25	355	741,38	1419,56	100,33	92,36	1,00	0,55	0,50	538,65	1280,02	1,91	1,11	
		460		1612,02			0,93	0,42	0,39	809,97	1551,35	2,17	1,04	
		690		1988,76			0,76	0,28	0,26	1230,67	1972,05	2,68	1,01	
	0,50	355		1868,40	97,64	92,36	1,00	0,53	0,50	820,49	1561,87	2,52	1,20	
		460		2199,36			0,93	0,41	0,39	1226,55	1967,93	2,97	1,12	
		690		2807,23			0,76	0,27	0,26	1855,57	2596,95	3,79	1,08	
10,00	0,25	355	1158,40	1651,26	154,71	142,42	1,00	0,76	0,70	304,05	1462,45	1,43	1,13	
		460		1822,70			0,93	0,59	0,54	592,72	1751,13	1,57	1,04	
		690		2176,15			0,76	0,39	0,36	1051,42	2209,82	1,88	0,98	
	0,50	355		2173,13	150,55	142,42	1,00	0,74	0,70	473,51	1631,92	1,88	1,33	
		460		2495,00			0,93	0,57	0,54	905,23	2063,64	2,15	1,21	
		690		3073,99			0,76	0,38	0,36	1590,45	2748,86	2,65	1,12	
12,00	0,25	355	1668,10	1951,57	219,82	202,42	1,00	>1,0	n.a.	n.a.	n.a.	n.a.	n.a.	
		460		2097,08			0,93	0,78	0,72	346,34	2014,44	1,26	1,04	
		690		2399,85			0,76	0,52	0,48	848,13	2516,23	1,44	0,95	
	0,50	355		2502,27	> f_{yf}	202,42	1,00	0,98	0,93	80,01	1748,11	1,50	1,43	
		460		2816,16			0,93	0,76	0,72	540,83	2208,93	1,69	1,27	
		690		3385,26			0,76	0,50	0,48	1289,78	2957,89	2,03	1,14	
15,00	0,25	355	2606,40	2412,02	> f_{yf}	> f_{yf}	1,00	n.a.	n.a.	n.a.	n.a.	n.a.	n.a.	
		460		2574,76			0,93	n.a.	n.a.	n.a.	n.a.	n.a.	n.a.	
		690		2850,77			0,76	n.a.	n.a.	n.a.	n.a.	n.a.	n.a.	
	0,50	355			> f_{yf}	> f_{yf}	1,00	n.a.	n.a.	n.a.	n.a.	n.a.	n.a.	n.a.
		460					0,93	n.a.	n.a.	n.a.	n.a.	n.a.	n.a.	
		690					0,76	n.a.	n.a.	n.a.	n.a.	n.a.	n.a.	

Table 3. Results obtained with the Beam-based model

4.3 Influence of the bearing length

The length of the stiff bearing device (s_s) is a variable that may undermine the application of the proposed formulation because its effect cannot be accounted for in simple beam models. This length is usually described as a percentage of distance a since it shows the degree of concentration the load has on the panel. The results summarized in Table 3 are plotted in figures 8 to 10. These figures suggest that the strength of slender girders to patch loading in which $t_w \leq 6$ mm, does not show a strong correlation with variations in the s_s/a ratio. For stocky girders in which $t_w > 6$ mm, it is observed that the greater the s_s/a ratio, the greater F_2/F_{Rk}^* ratio (safe side). Thus, the use of a beam model is preferred over a 3D FE GMNIA, because of its simplicity in terms of time computational time.

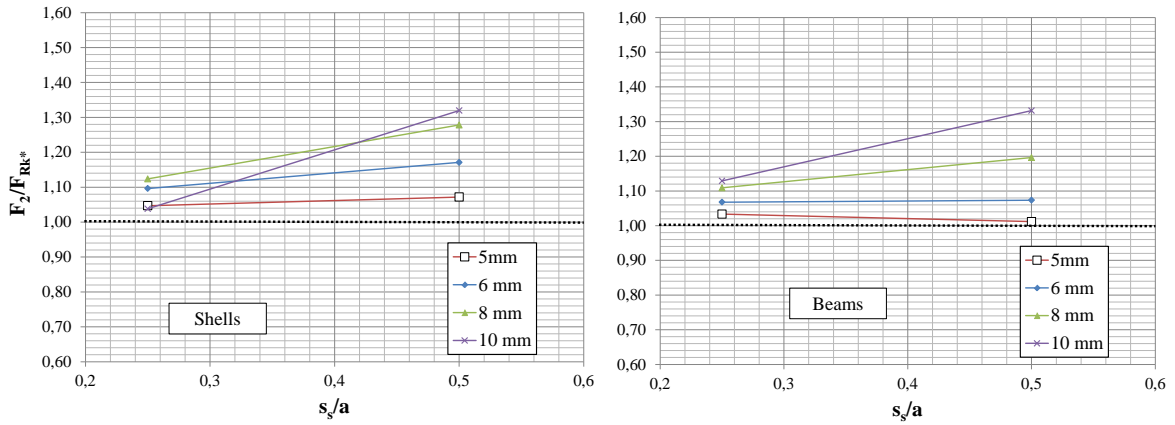


Figure 8. (F_2) vs- (F_{Rk}) ratios. $f_{yf}=355 \text{ N/mm}^2$ for shells (left) and beam (right) models

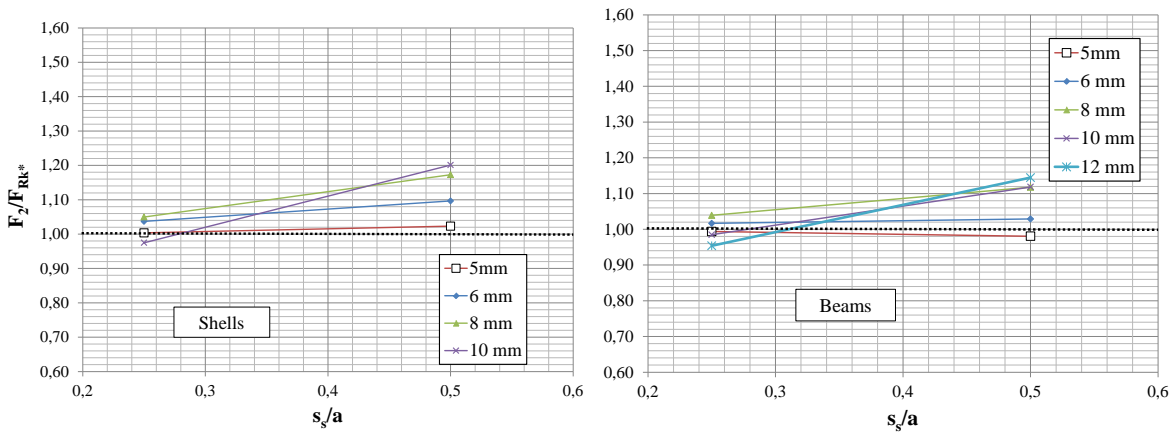


Figure 9. (F_2) vs- (F_{Rk}) ratios. $f_{yf}=460 \text{ N/mm}^2$ for shells (left) and beam (right) models

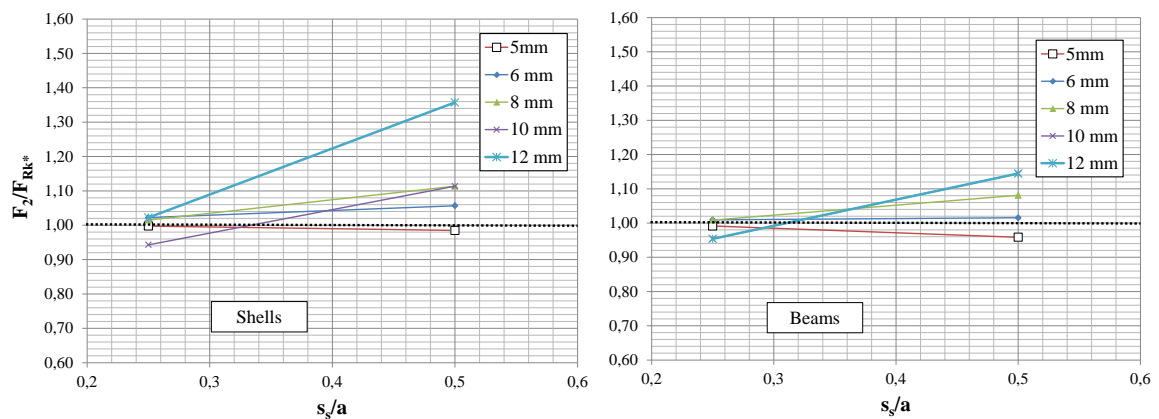


Figure 10. (F_2) vs- (F_{Rk}) ratios. $f_{yf}=690 \text{ N/mm}^2$ for shells (left) and beam (right) models

5. CASE STUDY

A case study of a notional composite bridge with plate girders is analyzed (Fig. 11). The approach spans are designed with pre-stressed concrete beams whereas the central beam is conceived with a series of composite concrete-steel plate girders. A realistic construction process may include the use of precast prestressed concrete girders and incremental launching of the plate girders. The focus of this study is the incremental launching process of the plate steel girders and in particular, the resistance to concentrated loading in unstiffened panels during launching.

The steel plate girders are launched from a working platform located on the left. The first span (between piers) and the cantilever (excluding the launching nose) are assumed as 25 meters long. An influence line analysis indicates that the vertical reaction of the system at the second pier (from left to right) is maximum, affecting an unstiffened cross-sections during launching. Figure 12 shows the proportions of the studied unstiffened panel. Plate girder proportions of this parametric investigation of the notional plate girder are summarized in Table 4. The values of t_w and f_{yf} correspond to those commercially available in plates.

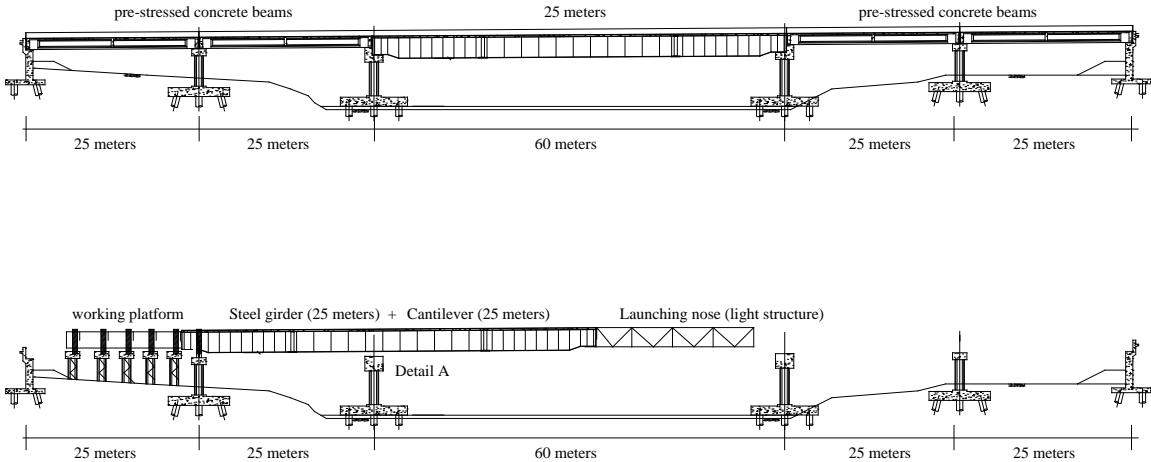


Figure 11. Case study. Final and temporary configuration during construction

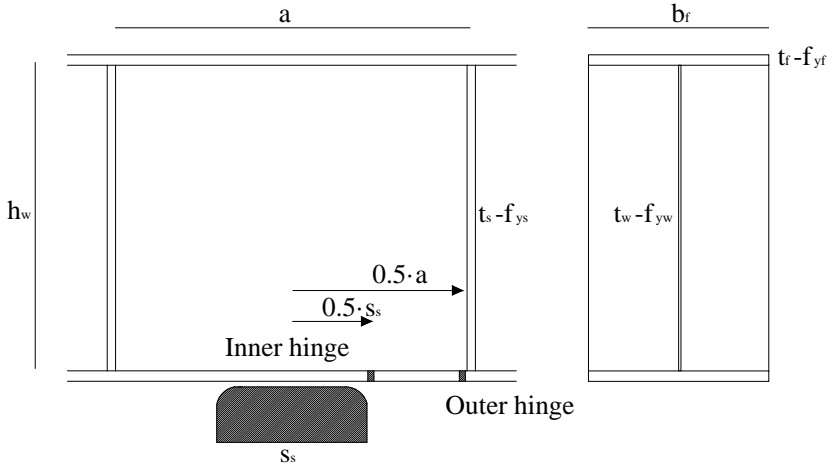


Figure 12. Studied panel (passing over the third support)

Model	t_w (mm)	t_f (mm)	f_{yw} (N/mm ²)	f_{yf} (N/mm ²)	a (mm)	s_s (mm)	h_w (mm)	b_f (mm)	m_1	m_2	I_y (mm)	$I_{y, corrected}$ (mm)	k_F	F_{cr} (kN)	F_y (kN)	λ_F	χ_F	F_{Rk} (EN1993-1-5) (kN)
1	10	60	355	355	2000	1000	1940	750	75,0	20,9	2295,2	2000,0	7,88	767,9	8147,9	3,26	0,15	1089,8
2	10	60	355	460	2000	1000	1940	750	97,2	20,9	2424,0	2000,0	7,88	767,9	8605,3	3,35	0,15	1060,4
3	10	60	355	690	2000	1000	1940	750	145,8	20,9	2669,3	2000,0	7,88	767,9	9475,9	3,51	0,14	1010,6
4	11	60	355	355	2000	1000	1940	750	68,2	20,9	2252,7	2000,0	7,88	1022,0	8796,6	2,93	0,17	1331,1
5	11	60	355	460	2000	1000	1940	750	88,3	20,9	2374,3	2000,0	7,88	1022,0	9271,7	3,01	0,17	1296,5
6	11	60	355	690	2000	1000	1940	750	132,5	20,9	2606,4	2000,0	7,88	1022,0	10178,0	3,16	0,16	1237,4
7	12	60	355	355	2000	1000	1940	750	62,5	20,9	2215,9	2000,0	7,88	1326,9	9439,9	2,67	0,19	1597,1
8	12	60	355	460	2000	1000	1940	750	81,0	20,9	2331,3	2000,0	7,88	1326,9	9931,4	2,74	0,18	1557,1
9	12	60	355	690	2000	1000	1940	750	121,5	20,9	2551,9	2000,0	7,88	1326,9	10871,2	2,86	0,17	1488,3
10	13	60	355	355	2000	1000	1940	750	57,7	20,9	2183,9	2000,0	7,88	1687,0	10078,6	2,44	0,20	1888,1
11	13	60	355	460	2000	1000	1940	750	74,8	20,9	2293,7	2000,0	7,88	1687,0	10585,4	2,50	0,20	1842,4
12	13	60	355	690	2000	1000	1940	750	112,1	20,9	2504,1	2000,0	7,88	1687,0	11556,6	2,62	0,19	1763,3
13	14	60	355	355	2000	1000	1940	750	53,6	20,9	2155,6	2000,0	7,88	2107,0	10713,5	2,25	0,22	2204,1
14	14	60	355	460	2000	1000	1940	750	69,4	20,9	2260,5	2000,0	7,88	2107,0	11234,6	2,31	0,22	2152,4
15	14	60	355	690	2000	1000	1940	750	104,1	20,9	2461,8	2000,0	7,88	2107,0	12235,3	2,41	0,21	2062,5
16	15	60	355	355	2000	1000	1940	750	50,0	20,9	2130,5	2000,0	7,88	2591,5	11344,9	2,09	0,24	2545,1
17	15	60	355	460	2000	1000	1940	750	64,8	20,9	2230,9	2000,0	7,88	2591,5	11879,4	2,14	0,23	2487,1
18	15	60	355	690	2000	1000	1940	750	97,2	20,9	2424,0	2000,0	7,88	2591,5	12908,0	2,23	0,22	2386,0
19	10	60	460	460	2000	1000	1940	750	75,0	20,9	2295,2	2000,0	7,88	767,9	10557,9	3,71	0,13	1240,5
20	10	60	460	690	2000	1000	1940	750	112,5	20,9	2506,0	2000,0	7,88	767,9	11527,8	3,87	0,13	1187,2
21	11	60	460	460	2000	1000	1940	750	68,2	20,9	2252,7	2000,0	7,88	1022,0	11398,4	3,34	0,15	1515,2
22	11	60	460	690	2000	1000	1940	750	102,3	20,9	2451,8	2000,0	7,88	1022,0	12406,3	3,48	0,14	1452,3
23	12	60	460	460	2000	1000	1940	750	62,5	20,9	2215,9	2000,0	7,88	1326,9	12232,0	3,04	0,16	1818,0
24	12	60	460	690	2000	1000	1940	750	93,8	20,9	2404,9	2000,0	7,88	1326,9	13275,3	3,16	0,16	1745,1
25	13	60	460	460	2000	1000	1940	750	57,7	20,9	2183,9	2000,0	7,88	1687,0	13059,6	2,78	0,18	2149,3
26	13	60	460	690	2000	1000	1940	750	86,5	20,9	2363,9	2000,0	7,88	1687,0	14136,0	2,89	0,17	2065,8
27	14	60	460	460	2000	1000	1940	750	53,6	20,9	2155,6	2000,0	7,88	2107,0	13882,2	2,57	0,19	2508,9
28	14	60	460	690	2000	1000	1940	750	80,4	20,9	2327,6	2000,0	7,88	2107,0	14989,6	2,67	0,19	2414,5
29	15	60	460	460	2000	1000	1940	750	50,0	20,9	2130,5	2000,0	7,88	2591,5	14700,4	2,38	0,21	2897,1
30	15	60	460	690	2000	1000	1940	750	75,0	20,9	2295,2	2000,0	7,88	2591,5	15836,9	2,47	0,20	2791,2

Table 4. EN1993-1-5 results for the case study

The optimization process starts by defining: i) a target load (action), ii) web height h_w , iii) web width a and iv) flange proportions, including width (b_f) and thickness (t_f), which calculated based on flexural requirements. Assuming a probable reaction (upper bound) of 2500 kN during launching, which accounts for uncertainties in the magnitude of loads over temporary supports during launching, several plate girders were proportioned. Table 4 shows 30 geometrical alternatives for given values of $h_w=1940$ mm $a=2000$ mm, $b_f=750$ mm and $t_f=60$ mm. Variations of f_{yw} , t_w and f_{yf} are addressed.

- The web thickness varies from $t_w=10$ mm to $t_w=15$ mm
- Two types of steel for the web of the plate girders are studied (S355 in models 1 to 18 and S460 in models 19 to 30).
- Webs made of S355 steel are combined with flanges made of S355, S460 and S690 steel, whereas the web of the S460 girder is combined with flanges made of S460 and S690 steel.

- The nominal strength based on the EN1993-1-5 specification is calculated for all cases. For all girders, l_y happens to be greater than the distance between stiffeners a .
- Note that only four girders, with web thickness 14 and 15 mm would be considered safe, of the 30 plate girders studied.
- Results from the analyses suggest that the homogeneous girders exhibit large load carrying capacity than their hybrid counterparts. Note that this observation penalizes the hybrid design.

Full 3D, FE GMNI (shell-based) simulations as well as results from simple hand calculations were conducted for the plate girder described in Table 4. Stresses in the beam flange were obtained from both modelling techniques at the inner and outer hinges (Fig 12). Note that the beam model assumes that the support is a point (and not roller or pad of finite dimensions). Results are summarized in Table 5. It is worth mentioning that for this case, hand calculations were performed over Euler-Bernoulli beams. As a result, the flange stresses are extracted from classical beam theory.

Results from the 3D FE GMNIA (F_2), suggest that the strength of all the girders exceeds 2500 kN, whereas the results from the proposed formulation (F_{RK*}), indicate that 25 of the 20 girders meet the strength requirement. To further investigate the potential cost-savings, the weight of the plate girders was normalized with respect to the weight of a plate girder with a web thickness of 15 mm. It is observed that the application of the simplified methodology to estimate the plate girder strength under patch loading based on a beam model, might lead to material savings of up to 25% for a plate girder in which the thickness is 11 mm. The application of the 3D FE GMNIA approach validates the use of a 10 mm thick web, which translates into a 31% in material savings.

The proposed methodology is particularly beneficial for the design of hybrid plate girders even if the penalizing factor k described in Eq. 8 is accounted for. Note that the numerical model shows that the strength F_2 strongly depends on the magnitude of f_{yf} .

Figure 13 shows the calculated strength ratios with the 3D FE GMNIA as a baseline comparison and as a function of the web slenderness ratio. Note that the EN1993-1-5 procedure significantly underestimates the strength of the web under patch loading and that the simplified proposal in which the stresses at in the flange are calculated based on classical beam theory, yield safe more accurate results than current the EN1993-1-5 provision.

Model	F_{Rk} (EN1993-1-5)	w (equivalent)	M_o (support + a/2)	M_i (support + a/2)	σ_o	σ_i	χ_o	χ_i	κ (hybrid)	ΔF_T	F_{Rk^*} (proposal)	F_2 (num)	Weight reduction
	(kN)	(kN/m)	(kN·m)	(kN·m)	(N/mm ²)	(N/mm ²)							
1	1089,8	20,5	5908,0	6156,7	61,1	63,7	0,34	0,35	1,00	1253,24	2343,0	3165,7	31,6%
2	1060,4	20,0	5748,8	5990,9	59,5	62,0	0,25	0,27	0,93	1313,66	2374,1	3564,5	31,6%
3	1010,6	19,0	5478,4	5709,0	56,7	59,1	0,16	0,17	0,76	1222,79	2233,3	4446,9	31,6%
4	1331,1	25,1	7215,9	7519,7	74,1	77,2	0,39	0,41	1,00	1147,90	2478,9	3406,1	25,3%
5	1296,5	24,4	7028,6	7324,5	72,2	75,2	0,30	0,31	0,93	1239,86	2536,4	3851,8	25,3%
6	1237,4	23,3	6708,3	6990,8	68,9	71,8	0,19	0,20	0,76	1183,67	2421,1	4733,9	25,3%
7	1597,1	30,1	8658,3	9022,8	88,3	92,1	0,45	0,47	1,00	1036,22	2633,4	3682,6	19,0%
8	1557,1	29,3	8441,4	8796,7	86,1	89,8	0,34	0,35	0,93	1161,55	2718,7	4123,1	19,0%
9	1488,3	28,0	8068,3	8407,9	82,3	85,8	0,22	0,22	0,76	1142,10	2630,4	4964,7	19,0%
10	1888,1	35,5	10235,8	10666,7	103,7	108,1	0,51	0,53	1,00	918,34	2806,5	3963,1	12,7%
11	1842,4	34,7	9987,8	10408,3	101,2	105,5	0,38	0,40	0,93	1078,83	2921,2	4368,0	12,7%
12	1763,3	33,2	9558,9	9961,4	96,9	100,9	0,25	0,26	0,76	1098,12	2861,4	5137,9	12,7%
13	2204,1	41,5	11948,7	12451,7	120,3	125,3	0,57	0,60	1,00	794,39	2998,5	4207,3	6,3%
14	2152,4	40,5	11668,3	12159,5	117,4	122,4	0,43	0,45	0,93	991,78	3144,1	4673,4	6,3%
15	2062,5	38,8	11180,9	11651,7	112,5	117,3	0,28	0,29	0,76	1051,79	3114,2	5276,9	6,3%
16	2545,1	47,9	13797,3	14378,2	138,0	143,8	0,64	0,67	1,00	664,49	3209,6	4456,9	0,0%
17	2487,1	46,8	13483,3	14050,9	134,8	140,5	0,48	0,50	0,93	900,49	3387,6	4828,4	0,0%
18	2386,0	44,9	12934,9	13479,5	129,3	134,8	0,31	0,32	0,76	1003,14	3389,1	5358,6	0,0%
19	1240,5	23,4	6725,2	7008,3	69,6	72,5	0,30	0,31	1,00	1728,43	2969,0	3775,3	31,6%
20	1187,2	22,3	6436,1	6707,0	66,6	69,4	0,19	0,20	0,88	1751,70	2938,9	4373,4	31,6%
21	1515,2	28,5	8214,0	8559,8	84,4	87,9	0,35	0,36	1,00	1608,51	3123,7	4065,1	25,3%
22	1452,3	27,3	7873,2	8204,7	80,9	84,3	0,22	0,23	0,88	1683,98	3136,3	4965,5	25,3%
23	1818,0	34,2	9856,0	10270,9	100,6	104,8	0,40	0,41	1,00	1481,39	3299,4	4429,9	19,0%
24	1745,1	32,8	9460,7	9859,0	96,5	100,6	0,25	0,26	0,88	1612,10	3357,2	5158,0	19,0%
25	2149,3	40,5	11651,6	12142,2	118,1	123,0	0,45	0,47	1,00	1347,21	3496,5	4719,1	12,7%
26	2065,8	38,9	11199,3	11670,7	113,5	118,3	0,29	0,30	0,88	1536,12	3602,0	5243,2	12,7%
27	2508,9	47,2	13601,4	14174,1	136,9	142,7	0,50	0,53	1,00	1206,11	3715,1	4750,6	6,3%
28	2414,5	45,4	13089,4	13640,5	131,8	137,3	0,32	0,34	0,88	1456,13	3870,6	5304,6	6,3%
29	2897,1	54,5	15705,7	16367,0	157,0	163,6	0,56	0,59	1,00	1058,24	3955,3	4799,3	0,0%
30	2791,2	52,5	15131,7	15768,8	151,3	157,7	0,36	0,38	0,88	1372,20	4163,4	5329,0	0,0%

Table 5. Numerical, EN1993-1-5 and proposed results for the case study

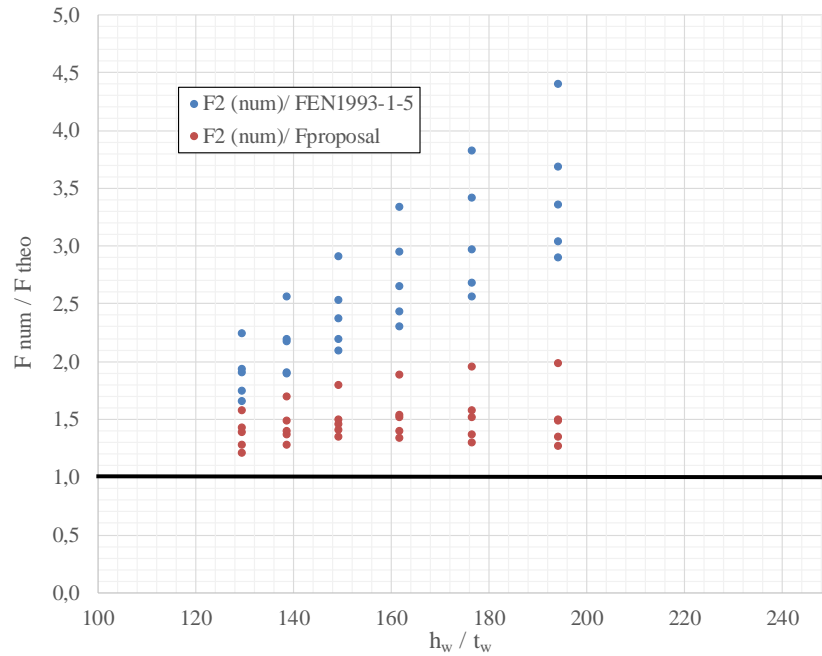


Figure 13. Numerical vs. Theoretical ratios for both the proposed and EN1993-1-5 formulations

6. CONCLUSIONS.

In this paper, a new formulation for steel plate girders subjected to patch loading is revisited from a practical perspective. The formulation is focused on the ultimate load capacity of steel plate girders subjected to patch loading, in the particular case of highly stiffened plates (transversally). Present versions of EN1993-1-5 include limitations in the formulae that generate discrepancies between engineering judgement, ultimate load capacity and stiffening philosophy, which suggest that in girders with transverse stiffeners, the closer these elements, the higher the ultimate load capacity. The present research includes the verification of an analytical formulation previously presented by one of the authors. Numerical studies using full GMNI analyses and simplified beams models are presented and compared. Multiple conclusions can be drawn from this study:

- In its present form, EN-1993-1-5 provisions for steel girders with closely spaced transverse stiffeners underestimate the ultimate load capacity observed both experimentally and numerically. The results obtained herein reinforce those derived by the first author in previous publications.
- The strength of the plate girder under patch loading can be obtained through simple hand calculation to obtain the stresses in the loaded flange due to bending.
- The beam model to obtain the stresses in the flange due to bending, in combination with the proposed procedure based on a yielding mechanism of the flanges to carry part of the patch load, provides straightforward procedure to estimate the strength of plate girders under concentrated loads, which may lead to considerable material savings, when compared to the application of the EN-1993-1-5 provision.
- The proposed formulation is particularly attractive for cases in which hybrid girders are used, even if the corresponding penalizing factors are used. In addition, the formulation is still valid for the case of the amended versions of I_y , accepted within the core of CEN/TC250/SC3, which is of special relevance for this structural type.

Future research studies related to this particular topic are suggested. The influence of longitudinal stiffening on the proposed formulation and/or the consideration of the defined load F_1 as a potential indicator of serviceability limit states are proposed.

References

- [1] EN1993-1-5. Eurocode 3. Design of steel structures – Part 1-5: Plated structural elements CEN. 2006
- [2] Roberts, T., Rockey, K., A mechanism solution for predicting the collapse loads of slender plate girders when subjected to in-plane patch loading, Proc. Inst. C. Eng., 67 (2). 155-175. 1979.

- [3] Lagerqvist, O., Johansson, B., Resistance of I-girders to concentrated loads. *Journal of Constr Steel Rsrch*, 39 (2). 87-119. 1996.
- [4] Graciano C., Lagerqvist O. Critical buckling of longitudinally stiffened webs subjected to compressive edge loads. *Journal of Constructional Steel Research*. Vol 59 (9): 1119-1149. 2003
- [5] Ren T., Gong GS., Elastic buckling of web plates in I-girders under patch and wheel loading *Engineering Structures*. Vol. 27(10):1528-1536. 2005
- [6] Kövesdi B., Dunai L. Bending, shear and patch loading interaction behaviour of slender steel sections. *Procedia Engineering*. Vol 156: 199:206. 2016
- [7] Kövesdi B., Alcaine J., Dunai L., Mirambell E., Braun B., Kulhmann U., Interaction behaviour of steel I-girders Part I: Longitudinally unstiffened girders. *Journal of Constructional Steel Research*. Vol. 103: 327-343. 2014
- [8] Graciano C., Ayestarán A., Steel plate girder webs under combined patch loading, bending and shear. *Journal of Constructional Steel Research*, 80 (1), pp 202 – 212, 2013
- [9] Navarro-Manso A., del Coz Días J., Alonso-Martínez M., Blanco-Fernandez E., Castro-Fresno D., New launching method for steel bridges based on a self-supporting deck system: FEM and DOE analyses. *Automation in Construction*. Vol 44, pp 183-196. 2014
- [10] Navarro-Manso A., del Coz Días J., Alonso-Martínez M., Castro-Fresno D., Alvarez Rabanal F., Patch loading in slender and high depth steel panels: FEM–DOE analyses and bridge launching application. *Engineering Structures*. Vol.83:74-85. 2015
- [11] Chacón R., Mirambell E., Real E. Transversally stiffened plate girders subjected to patch loading. Part 1. Preliminary study. *Journal of Constructional Steel Research*. 80 (1), pp 483-491. 2013
- [12] Chacón R., Mirambell E., Real E. Transversally stiffened plate girders subjected to patch loading. Part 2. Additional numerical study and design proposal. *Journal of Constructional Steel Research*. 80 (1), pp 492-504. 2013
- [13] Chacón R., Mirambell E., Real E. Influence of flange strength on transversally stiffened girders subjected to patch loading. *Journal of Constructional Steel Research*. Vol. 97: 39-47. 2014
- [14] Graciano C. Patch loading resistance of longitudinally stiffened girders. A systematic review. *Thin-Walled Structures*. Vol. 95, 1-6. 2015.
- [15] Graciano C., Uribe-Henao A., Strength of Steel I.Girders subjected to eccentric patch loading. *Engineering Structures*. Vol. 79(15), 401-406. 2014
- [16] Cevik A., Göğus MT., Guzelbey I., Filiz H. A new formulation for longitudinally stiffened webs subjected to patch loading using stepwise regression method. *Advances in Engineering Software*. Vol 41(4), 611-618. 2010

[17] Chacón, R., Braun B., Kuhlmann U., Mirambell E. Statistical evaluation of the new resistance model of steel plate girders subjected to patch loading. *Steel Construction*. Vol 5 (1). 2012

[18] Abaqus Simulia, Dassault Systèmes (2016).

[19] Chacón, Mirambell Real. Influence of designer-assumed initial conditions on the numerical modelling of Steel plate girders subjected to patch loading. *Thin-Walled Structures*. Vol. 47(4): 391-402. 2009

[20] BSK 99. Boverkets handboken om stålkonstruktioner, Boverket. 1999 (in Swedish)